BIOCHEMISTRY
including biophysical chemistry & molecular biology
Article

Biochemistry **2010,** *49,* 709–717 709
DOI: 10.1021/bi901495y

Activation of Retinal Guanylyl Cyclase RetGC1 by GCAP1: Stoichiometry of Binding and Effect of New LCA-Related Mutations†

Igor V. Peshenko,‡ Elena V. Olshevskaya,‡ Suxia Yao,§ Hany H. Ezzeldin,§ Steven J. Pittler,§ and Alexander M. Dizhoor*,‡

‡*Hafter Research Laboratories, Pennsylvania College of Optometry, Salus University, Elkins Park, Pennsylvania 19027 and* §*Department of Vision Sciences, University of Alabama, Birmingham, Alabama 35294*

Received August 26, 2009; Revised Manuscript Received November 23, 2009

ABSTRACT: Retinal membrane guanylyl cyclase (RetGC) and Ca^{2+}/Mg^{2+} sensor proteins (GCAPs) control the recovery of the photoresponse in vertebrate photoreceptors, through their molecular interactions that remain rather poorly understood and controversial. Here we have determined the main RetGC isozyme (RetGC1):GCAP1 binding stoichiometry at saturation in cyto, using fluorescently labeled RetGC1 and GCAP1 coexpressed in HEK293 cells. In a striking manner, the equimolar binding of RetGC1 with GCAP1 in transfected HEK293 cells typical for wild-type RetGC1 was eliminated by a substitution, D639Y, in the kinase homology domain of RetGC1 found in a patient with a severe form of retinal dystrophy, Leber congenital amaurosis (LCA). A similar effect was observed with another LCA-related mutation, R768W, in the same domain of RetGC1. In contrast to the completely suppressed binding and activation of RetGC1 by Mg^{2+}-liganded GCAP1, neither of these two mutations eliminated the GCAP1-independent activity of RetGC stimulated by Mn^{2+}. These results directly implicate the D639 (and possibly R768)-containing portion of the RetGC1 kinase homology domain in its primary recognition by the Mg^{2+}-bound activator form of GCAP1.

Ca^{2+}-sensitive membrane guanylyl cyclase (RetGC)[1] plays a key role in regulation of the photoresponse in a vertebrate retina (reviewed in ref *1*). Absorption of light by visual pigments in rods and cones triggers activation of the transducin-PDE6 cascade, thus reducing free cGMP levels in the outer segment and closing cGMP-gated channels. The interruption of Na^+ and Ca^{2+} influx through the channels consequently causes hyperpolarization of the photoreceptor plasma membrane and interrupts the release of neuromediator from their synaptic terminals. Rods and cones recover from excitation and regain their light sensitivity by both inactivating the PDE6 cascade and resynthesizing cGMP by RetGC; the latter reaction is controlled via a Ca^{2+} feedback mechanism (*2*, *3*) by Ca^{2+}/Mg^{2+} binding proteins, GCAPs (guanylyl cyclase activating proteins) (*4*−*7*). Because Ca^{2+} influx stops in the light, its concentration in the outer segment falls nearly 10-fold (*8*, *9*). In response to this change, GCAPs are converted from their Ca^{2+}-bound (inhibitor) state to the Mg^{2+}-bound (activator) state and boost the catalytic activity of RetGC (*10*, *11*). Two RetGC isozymes, RetGC1 and RetGC2 (*12*−*14*), have been found in rods and cones. While RetGC1 is the main GCAP-regulated isozyme (*6*, *15*) and is essential for the survival of cones (*13*), both isozymes are required for the normal photoresponse in rods (*14*). Two isoforms of GCAPs (GCAP1 and GCAP2), ubiquitous among vertebrates (*5*, *6*, *16*, *17*), together provide the normal recovery speed in mouse rods (*3*, *11*, *18*), but additional GCAP isoforms have also been found in a variety of vertebrate species (*19*, *20*). Despite significant progress in understanding how GCAPs mediate the Ca^{2+} feedback loop of RetGC activity (*11*, *19*), some key intricate processes involved in the GCAP−RetGC interaction remain unclear, including the stoichiometry of the GCAP−RetGC complexes and the interaction between amino acid residues in RetGC and GCAPs responsible for cyclase activation.

A number of mutations in RetGC1 that alter its activity and/or regulation by GCAPs have been linked to blinding disorders in humans. These mutations can be divided in two major types: the loss-of-function mutations that result in the absence of RetGC1 activity and are frequent among patients with Leber congenital amaurosis (LCA) (*21*−*26*) and gain-of-function mutations associated with congenital dominant cone−rod dystrophy, CORD6 (*27*, *28*), that decrease the Ca^{2+} sensitivity of the GCAP−RetGC1 complex, thus possibly leading to an abnormal increase in the level of cGMP production in photoreceptors in the dark (*29*−*31*). Disease-related mutations that alter interactions of RetGC and GCAPs can help not only explain the cause of congenital blindness but also elucidate the mechanisms of GCAP−RetGC interactions. In this paper, we present evidence that the stoichiometry of a GCAP1−RetGC1 complex produced in HEK293 cells is 1:1 and describe that two new mutations found in patients with LCA completely prevent formation of the RetGC1−GCAP1 complex by blocking GCAP1 docking on RetGC1.

EXPERIMENTAL PROCEDURES

Recombinant GCAP1. GFP-tagged bovine GCAP1 was expressed in HEK293 cells from a Clontech pQBI25-fN3 vector

†This work was supported by National Institutes of Health Grants EY11522 (A.M.D.) and EY09924 and EY018143 (S.J.P.), Foundation Fighting Blindness (S.J.P.), the Pennsylvania Department of Health, and Pennsylvania Lions Sight Conservation and Eye Research Foundation (A.M.D.). A.M.D. is the Martin and Florence Hafter Professor of Pharmacology.

*To whom correspondence should be addressed: Pennsylvania College of Optometry, 8360 Old York Rd., Elkins Park, PA 19027. Telephone: (215) 780-1468. Fax: (215) 780-1464. E-mail: adizhoor@salus.edu.

[1]Abbreviations: DIC, differential interference contrast; EGTA, ethylene glycol bis(2-aminoethyl ether)-*N*,*N*,*N*′,*N*′-tetraacetic acid; GCAP, guanylyl cyclase activating protein; GFP, green fluorescent protein; LCA, Leber congenital amaurosis; MOPS, 4-morpholinopropanesulfonic acid; RetGC, photoreceptor membrane guanylyl cyclase.

Published on Web 01/05/2010

as described previously (*32*). Recombinant myristoylated wild-type GCAP1 was expressed in *Escherichia coli* and purified as described previously (*33*).

Screening for RetGC1 Mutations in LCA Patients. Three affected individuals whose DNA was analyzed in this study present with typical Leber congenital amaurosis (OMIM #204000). In the case of the D639Y mutation, two affected individuals carrying the mutation were siblings; their mother, who was also heterozygous for the mutation, exhibited subclinical changes in cone ERG but was otherwise unremarkable. The R768W mutation was a simplex case, and no further information about the patient or the family is available. DNA was isolated from peripheral blood samples obtained with informed consent by J. Nathans (Johns Hopkins University, Baltimore, MD) and B. Falsini (Università del Cattolica Sacro Cuore, Rome, Italy).

(*i*) *PCR Optimization with Epicentre FailSafe System*. Amplification reactions were optimized with FailSafe PCR 2× PreMixes A-L (Epicentre Technologies). Amplification reactions for each exon of the GC1 gene were conducted using the manufacturer's protocol in 25 μL reaction volumes for 35 cycles with an initial denaturation step of 5 min at 94 °C, and a final extension for 7 min at 72 °C. FailSafe buffer F for exon 12 and buffer I for exon 9 were used. The annealing temperature was 55 °C for exon 9 and 60 °C for exon 12. Amplification of exon 9 was conducted with forward primer 5′-CCCACATTGCCCTGGGCAGA and reverse primer 5′-CCTGCCCCCAGGACGTCACC generating a 204 bp product; amplification of exon 12 was conducted with forward primer 5′-GGCAGCCTTTGTGTTCTGGG and reverse primer 5′-GTTGCTGACAAGCATTTGGG generating a 267 bp product.

(*ii*) *Denaturing High-Pressure Liquid Chromatography* (*HPLC*). Mutation detection was conducted using the Transgenomic WAVE DNA Fragment Analysis System. For run parameter optimization, each PCR fragment (200 μL of unpurified "wild-type" PCR product) was denatured for 5 min at 95 °C and gradually reannealed with a decrease in sample temperature from 95 to 25 °C over a period of 45 min. The reannealed products were analyzed via injection of 5 μL on a linear gradient of 65% buffer A [0.1 M TEAA (pH 7.0)] and 35% buffer B (0.1 M TEAA and 25% acetonitrile) with a 2% change in slope per minute and a total acquisition time of 18.8 min at a flow rate of 0.9 mL/min at 50 °C. From the retention time, an optimized gradient was calculated to set peak elution at around 6−6.5 min. Additionally, 3 μL of PCR product was repeatedly injected for temperature titration over the range from 50 to 70 °C using the optimized gradient. The optimized gradient ranged from 46 to 57% buffer B with a total acquisition time of 10 min and melting temperatures ranging from 60 to 68 °C for all GC1 exons.

(*iii*) *DNA Sequencing of PCR Products*. PCR products that displayed an altered migration were cycle sequenced using Sequitherm Excel II with end-labeled primers and analyzed on a Genomyx LR DNA Sequencer (Beckman Coulter). All products were sequenced on both DNA strands, and more than one independent PCR product was sequenced for confirmation.

Generation of Plasmids Carrying Engineered RetGC1 Alleles. A pRCCMV plasmid carrying wild-type (WT) RetGC1 (*34*) was mutated using the Stratagene QuikChange site-directed mutagenesis kit according to the manufacturer's protocol. Plasmid sequence was verified on both strands for the entire RetGC1 cDNA contained in the plasmid.

Recombinant dsRed-Tagged RetGC1 and dsRed-RetGC1−GCAP1-GFP Chimera. Fluorescently labeled RetGC1 was produced via insertion into RetGC1 cDNA of a DNA fragment encoding a monomeric variant of red fluorescent protein (m-DsRed, Clontech), as described previously (*32*). The resultant construct, dsRed-RetGC1 pRCCMV, was used to express functional fluorescently tagged RetGC1 in HEK293 cells. To produce the dsRed-RetGC1−GCAP1-GFP "chimera", the GCAP1-GFP sequence was PCR-amplified by PFU polymerase (Stratagene) from a DNA clone used for expression of GCAP1-GFP in HEK293 cells (*32*) using a forward primer (5′-AAAAAA-CGGCCGATGGGGAACATTATGAGCGGTAAGTCG-3′) and a reverse primer (5′-gccaacgcgtctagatagtcaatcgatg-3′), thus adding EagI and XbaI restriction sites at the ends of the PCR product. The PCR product was then inserted into the EagI and XbaI sites of the dsRed-RetGC1 pRCCMV construct. All constructs were verified by automated DNA sequencing. Recombinant RetGC1 was expressed in HEK293 cells from a modified pRCCMV vector (Stratagene), as previously described (*10*).

Antibodies. Anti-RetGC1 antibodies were produced in rabbits against large recombinant fragments of human RetGC1 (*34*), Met747−Ser1052 (antibody RetGC1Cat) or Arg540−Asn815 (antibody RetGC1KHD), expressed in *E. coli* from the pET15b vector (Novagen/Calbiochem). The IgG fraction was purified using Protein A-Sepharose (GE Healthcare). The anti-GCAP1 polyclonal antibody was produced as described in ref *32*. Commercial antibodies against c-myc tag, dsRed, and GFP were purchased from Millipore, Clontech, and Invitrogen, respectively. Secondary peroxidase-conjugated antibodies were from Pierce/Thermo Scientific and Alexa Fluor 568 goat anti-rabbit antibody from Molecular Probes/Invitrogen.

Expression of RetGC1 in HEK293 Cells. HEK293 cells were grown at 37 °C, 5% CO_2, in high-glucose Dulbecco's modified Eagle's medium (DMEM, Invitrogen) supplemented with 10% fetal bovine serum (Invitrogen). To express RetGC1 and its mutants for the functional assay in vitro, HEK293 cells were transfected with 40 μg/100 mm culture dish of pRCCMV plasmid containing wild-type or mutant RetGC1 using the Ca^{2+} phosphate method (a Promega Profection protocol), and the membranes were harvested as previously described (*31*). In coexpression experiments, HEK293 cells were typically transfected with 40 μg of an equimolar mixture of pRCCMV plasmids containing ΔRetGC1 and mutant RetGC1 per dish using the same protocol. The expression level of each protein was determined by immunoblot using the rabbit polyclonal anti-RetGC1Cat antibody.

Coexpression of RetGC1 and GCAP1 in HEK293 Cells and Confocal Laser Scanning Microscopy. Cells were grown in standard glass coverslip chambers (four 2 cm^2 chambers per slide) in Dulbecco's modified Eagle's medium supplemented with 10% fetal bovine serum and were transfected with a mixture of expression constructs using the Ca^{2+} phosphate method. Routinely, a mixture of 3 μg of pRCCMV plasmid containing wild-type or mutant RetGC1 cDNA and 0.02 μg of the GCAP1-GFP pQBI25fN3 plasmid (*32*) was used per chamber. In 24−32 h, we either directly viewed the live cells or fixed them with freshly prepared 4% paraformaldehyde in a standard Tris-buffered saline (TBS) at room temperature for subsequent immunostaining (*32*). Where indicated, the DNA in nuclei of the cells was counterstained for 10 min with 1 mM TO-PRO-3 iodide (Invitrogen) containing 20 μg/mL RNase A added to the first wash following the incubation with the secondary antibody and then washed as described above.

The cells were viewed using an inverted Olympus IX81 microscope/FV1000 Spectral laser confocal system, and images were collected and analyzed using Olympus FluoView FV10-ASW.

To determine the stoichiometry of binding of GCAP1 to RetGC1, the HEK293 cells in the neighboring chambers of the same coverslip were transfected with 3 μg of pRCCMV plasmid containing the monomeric dsRed-RetGC1−GCAP1-GFP chimera cDNA or a mixture of 3 μg of the dsRed-RetGC1 construct and 0.02−0.6 μg of the GCAP1-GFP pQBI25fN3 plasmid. All cells were viewed, and fluorescence intensity profiles were recorded at the same laser excitation and photomultiplier gain settings.

Immunoblotting and Immunoprecipitation. HEK293 membrane fractions were washed in TBS and dissolved in a Laemmli SDS−PAGE sample buffer, and aliquots were separated via 4 to 12% PAGE (Invitrogen) or 7% PAGE. Following electroblotting on an Immobilon P membrane (Millipore), proteins were probed with antibodies and developed using a Pierce Femto Supersignal luminescent peroxidase substrate, according to the manufacturer's protocol. The signal intensity was quantified with densitometry X-ray film as previously described (*32*) or using a LuminousFX imaging system (FotoDyne, Inc.).

Immunoprecipitation. Approximately 30 μL of each membrane fraction containing expressed RetGC1 mutants was dissolved for 15 min at room temperature in 200 μL of extraction buffer [20 mM Tris-HCl (pH 7.5), 1.5% Triton X-100, 500 mM KCl, 10 mM NaCl, and 1 mM $MgCl_2$] supplemented with 0.5 mg/mL bovine serum albumin and centrifuged at 10000 rpm for 5 min. The supernatant was collected, mixed with 5 μg of anti-Myc IgG, incubated for 30 min, mixed with 100 μL of a protein A-Sepharose suspension equilibrated with extraction buffer (set bed volume of ~20 μL), and incubated for an additional 15 min with constant agitation. The beads were then centrifuged at 2000 rpm for 2 min, washed in 1 mL of extraction buffer, collected at 2000 rpm for 2 min, and washed once in 50 mM Tris (pH 6.8) containing 1 mM $MgCl_2$. The beads collected by centrifugation were resuspended in 80 μL of 2× Laemmli SDS sample buffer and removed by centrifugation at 10000 rpm for 1 min. The supernatant was analyzed via electrophoresis in 7% PAAG-SDS and immunoblotting using RetGC1Cat antibody.

Guanylyl Cyclase Activity. RetGC activity was assayed as previously described (*10*, *32*). Briefly, the assay mixture (25 μL) contained 30 mM MOPS-KOH (pH 7.2), 60 mM KCl, 4 mM NaCl, 1 mM DTT, 1 mM free Mg^{2+}, 2 mM Ca/EGTA buffer, 0.3 mM ATP, 4 mM cGMP, 1 mM GTP, 4 mM creatine phosphate, 0.5 unit of creatine phosphokinase, 1 μCi of [α-^{32}P]GTP, 0.1 μCi of [8- ^{3}H]cGMP, GCAP1, and HEK293 cell membranes. The reaction mixture was incubated for 40 min at 30 °C; we stopped the reaction by heating the mixture for 2.5 min at 95 °C, and aliquots were analyzed by TLC on fluorescent plastic-backed polyethylenimine cellulose plates (E. Merck) as described previously (*10*, *35*). The data shown are representative of three to four independent experiments producing virtually identical results.

RESULTS AND DISCUSSION

Mutations in the chromosome 17p13.1 GUCY2D locus encoding RetGC1 have been frequently found in patients with LCA (*21*, *22*, *24*, *25*, *36*). Therefore, we verified the sequence of

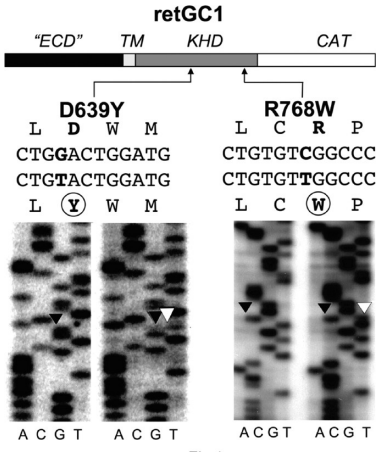

FIGURE 1: Mutations identified in exon 9 and exon 12 of GUCY2D in LCA patients. Analysis of exon 12 revealed a C → T nucleotide change resulting in an R768W mutation. In exon 9, a G → T nucleotide change results in a D639Y mutation. The sequence changes were not observed in more than 100 control samples that were analyzed. For each sequencing reaction set, the control is on the left and the LCA patient sequence is on the right. The positions of the mutated amino acid residues in the primary structure are indicated in the schematics of the conventional RetGC1 domain map: *ECD*, extracellular domain; *TM*, transmembrane domain; *KHD*, kinase homology domain; *CAT*, catalytic domain.

RetGC1 in new LCA patients as a likely link to the onset of the disease. Screening results in DNA of two LCA patients revealed two mutations: D639Y, a novel sequence change, and R768W (*37*), both in the kinase homology domain (KHD) of RetGC1 (Figure 1). In each case, however, each mutant allele was heterozygous both in patients and in one of the parents (see Experimental Procedures). This finding seemingly reduced the likelihood of a direct role of the two mutants alone in the development of the retinal degeneration, because the LCA symptoms evident in each patient were not observed in their parents; however, one parent carrier (D639Y) was shown to exhibit subclinical cone ERG changes, and ERG changes have been reported previously in other LCA carriers (*38*). Thus, the possibility remained that the mutant RetGC1 could contribute to the LCA through additional, presently unclear, genetic interaction(s), if its normal function was altered by the mutations. Therefore, we tested the activity and regulation of the mutant RetGC1 by GCAPs for any evidence for such abnormalities. We expressed the D639Y and R768W RetGC1 mutants in HEK293 cells and tested their activation by purified recombinant GCAP1 in vitro (Figure 2). As controls, we used wild-type recombinant human RetGC1 and another RetGC1 mutant, R838S, that is linked to dominant cone−rod degeneration (*27*, *30*) through increased affinity for Mg^{2+}-bound GCAP1 (*31*) causing abnormal Ca^{2+} sensitivity of RetGC1. All variants of RetGC1 used in this assay were present in similar quantities equalized by polyclonal anti-RetGC1Cat antibody staining (Figure 2C). The antibody was produced against a large 30 kDa fragment of RetGC1 containing the catalytic domain (*34*) and therefore would unlikely be sensitive to single-point mutations (of which the D639Y mutation was located >100 amino acid residues upstream of the region recognized by the antibody).

Both the D639Y and R768W mutations drastically changed the enzymatic properties of RetGC1 (Figure 2). Whereas the wild type and the R838S RetGC1 demonstrated a robust stimulation by GCAP1, D639Y RetGC1and R768W RetGC1 failed to show

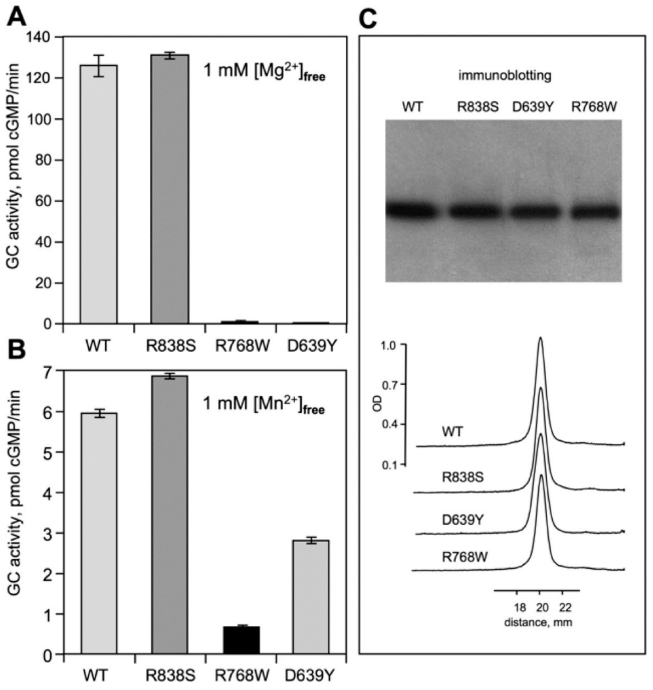

FIGURE 2: Effect of D639Y and R768W mutations on the GC activity of RetGC1. (A and B) Recombinant WT RetGC1 and its mutants present in HEK293 membrane fraction were assayed for guanylyl cyclase activity in the presence of 1 mM free Mg^{2+}, 10 μM GCAP1, and 2 mM EGTA (A) or 5 mM Mn^{2+} (B). The activities are standardized for the RetGC1 content in each assay, equalized with the wild type as a standard. The average of three independent measurements is shown. For other conditions of the assay, see Experimental Procedures. (C) Immunoblot probed with anti-RetGC1Cat antibody and analyzed by densitometry used to equalize the RetGC1 content between the HEK293 membrane preparations.

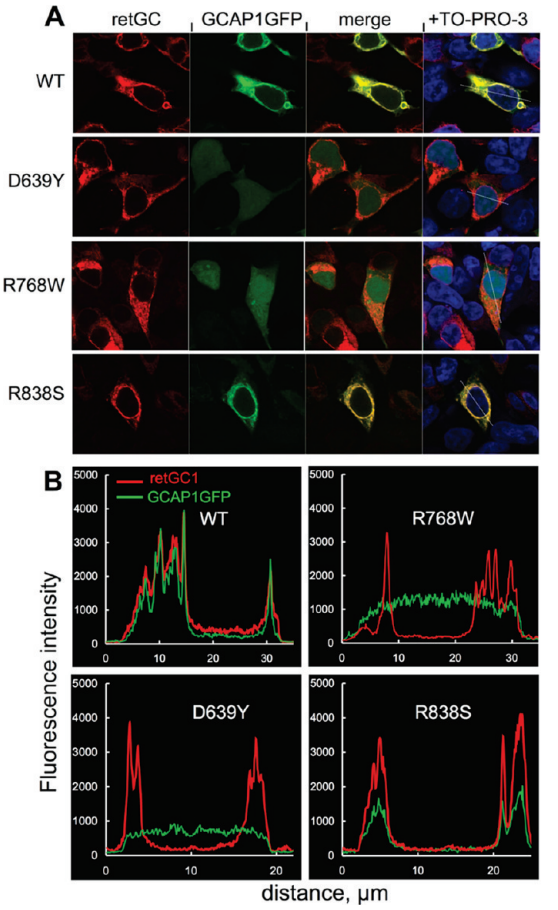

FIGURE 3: Cellular localization of GCAP1-GFP coexpressed with RetGC1 mutants. (A) Fluorescence of GCAP1-GFP and RetGC1 (anti-RetGC1KHD primary and Alexa Fluor 568 secondary antibody) in HEK293 cells coexpressing GCAP1-GFP and wild-type (WT) or mutant RetGC1 (D639Y, R768W, and R838S mutants). The first two columns show GCAP1-GFP and Alexa Fluor 568 fluorescence, respectively. The third column shows the merged fluorescence images in the first two columns. The right-most panels show the merged images counterstained with TO-PRO-3 (pseudo blue). The GFP fluorescence of GCAP1-GFP was excited at 488 nm and the anti-RetGC1KHD−Alexa Fluor 568 antibody complex at 543 nm. The cells were fixed with 4% paraformaldehyde. For other details, see Experimental Procedures. (B) Representative fluorescence intensity profiles recorded from the cells expressing GCAP1-GFP and wild-type or mutant RetGC1 shown in panel A along the lines superimposed on the merged fluorescent images shown in the right-most panels in panel A.

any activation even at saturating concentrations of wild-type GCAP1 (Figure 2A). The lack of activity was unlikely due to a nonspecific inactivation of the mutant cyclase, because both D639Y and R768W RetGC1 displayed reduced but readily detectable GCAP-independent basal activity in the presence of Mn^{2+} (Figure 2B). The reduction in basal activity was by far less severe than the complete lack of the GCAP1-dependent activity, especially for the D639Y mutant, which retained nearly half the normal level of basal activity. Therefore, the more likely explanation could be one of the following. (i) The mutant cyclases were unable to bind GCAP1, or (ii) the cyclase mutants were capable of binding GCAP1, but failed to increase their catalytic activity, because some potential secondary interactions in the GCAP1−RetGC1 complex failed to properly occur.

To assess the efficiency of binding of GCAP1 to D639Y and R768W RetGC1, we utilized our recently described cell-based assay using RetGC1 and GCAP1-GFP coexpression in HEK293 cells (*32*) (Figure 3). While GCAP1-GFP expressed alone always shows a diffuse uniform distribution throughout the cytoplasm and the nucleus, when coexpressed with RetGC1 it colocalizes with the cyclase in the membranes of the endoplasmic reticulum and to a much lesser extent in the plasma membrane, thus forming a characteristic "donuts and tennis rackets" pattern (*32*). Such a colocalization pattern was observed in our experiments with both wild-type and R838S RetGC1 (Figure 3A), with the across-the-cell profile of GCAP1 fluorescence matching that of the anti-RetGC1 immunofluorescence (Figure 3B). In striking contrast, GCAP1-GFP coexpressed with either D639Y or R768W RetGC1 remained diffusely distributed through the entire cell, thus showing no evidence for binding to the cyclase. The levels of expression of both RetGC1 and GCAP1-GFP unavoidably vary between different cells, even in the same culture sample (*32*). Therefore, for more accurate semiquantitative characterization of the ability of the cyclase to bind GCAP1, we determined the ratio between the maximal GFP fluorescence intensity in the whole cell and its maximal fluorescence intensity inside the nucleus (Figure 4). For GCAP1-GFP expressed without the cyclase, this ratio is close to 1.0 but sharply increases after cotransfection with RetGC1, reflecting depletion of GCAP1 from the nucleus due to compartmentalization with the cyclase in the membranes (*32*). Whereas for both wild-type and R838S RetGC1 the GCAP1 clearance between the membranes and the nucleus averaged from a random sample of cells from the same culture rose near 10-fold compared with that of GCAP1-GFP expressed alone, it remained close to 1 for both the R639Y and R768W mutants. The difference from wild-type and R838S

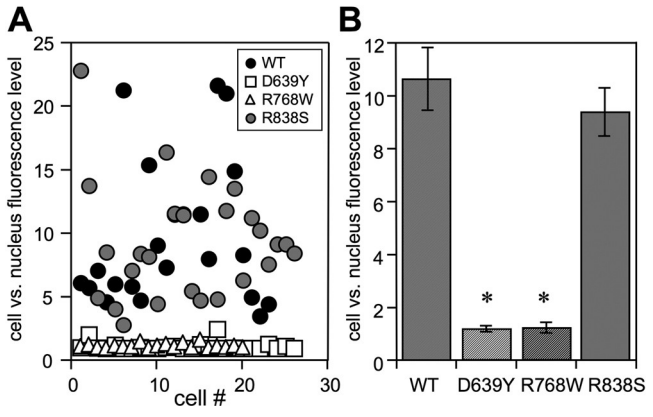

FIGURE 4: Effect of RetGC1 mutations on GCAP1-GFP colocalization with RetGC1. (A) Cell:nucleus GCAP1-GFP fluorescence intensity ratio among the HEK293 cells that coexpress GCAP1-GFP with WT (●), D639Y (□), R768W (△), and R838S (gray circles) RetGC1. The cell:nucleus fluorescence intensity ratio is the ratio of the maximal GFP fluorescence intensity in the whole cell to its maximal fluorescence intensity inside the nucleus. Each point represents a single cell. (B) Average ratio (mean ± standard error, cell number) for GCAP1-GFP coexpressed with WT (10.6 ± 1.4; $n = 25$), D639Y (1.2 ± 0.1; $n = 26$), R768W (1.2 ± 0.04; $n = 20$), and R838S (9.3 ± 0.9; $n = 26$) RetGC1. An asterisk indicates $p < 0.01$ vs the wild type.

RetGC1 was statistically highly significant (ANOVA/Bonferroni post hoc test, $p < 0.01$, confidence limit of 99%). Hence, the lack of activity for both R639Y and R768W can be explained primarily by the loss of their affinity for GCAP1.

Does this mean that each mutant cyclase has just a smaller number of GCAP1 molecules associated with it or that GCAP1 simply does not bind to RetGC1? The answer depends on how many molecules of GCAP1 are actually associated with the cyclase at saturation, one or many. Although the levels of expression for RetGC1 and GCAPs are both estimated to be in the micromolar range (*38*), the exact stoichiometry between GCAP1 and RetGC1 in their complex is unknown. To resolve this question, we estimated the ratio between GCAP1 and RetGC1 using GCAP1-GFP and RetGC1 fluorescently tagged by replacing a portion of the cyclase ECD domain with monomeric dsRed red fluorescent protein (*32*). Neither of these modifications critically affected RetGC1 activity or its affinity for GCAP1 (*32*). To normalize the fluorescence of both tags in the membranes of cotransfected cells relative to a 1:1 molar ratio of the GCAP1-GFP−dsRed-RetGC1 complex, we produced the "1:1 standard chimera" in which GCAP1-GFP was directly fused with dsRed-RetGC1 in a single ~170 kDa chimera protein that contained both fluorescent tags (Figure 5A and Figure 1S of the Supporting Information). The ratio between the green and red tag fluorescence brightness for the 1:1 chimera was calculated by dividing the average value of the green fluorescence in the cell by the average value of red fluorescence in the same region of the cell. The average ratio determined from many cells measured in this experiment was 1.87 ± 0.04 (mean ± standard error of the mean; $n = 75$). It also needs to be noted that there is a distinct cell-to-cell variability in the same cell culture, which could appear somewhat surprising in the case of a single polypeptide containing both tagged proteins (Figure 1S of the Supporting Information). One possible explanation is that perhaps a small variation in fluorescent tag folding or maturation exists between different cells in the same population. Therefore, a large number of cells were included in the analysis to average out the cell-to-cell variations.

We then measured the fluorescence of the two tags in the cells that coexpressed individual dsRed-RetGC1 and GCAP1-GFP species using the same settings for fluorescence excitation and image acquisition that we used for the 1:1 chimera as a standard. In our previous experiments, the cell-based binding assay was normally conducted at GCAP1-GFP:RetGC1 cDNA ratios as low as 1:150 to prevent RetGC1 from being saturated by GCAP1. Under those conditions, there was a 10−20-fold molar excess of RetGC1 over GCAP1 (*32*). Consequently, almost all GCAP1 was associated with the membrane-bound RetGC1, and very little, if any, of the green fluorescence could be detected in the nuclei. However, to evaluate the stoichiometry for the GCAP1−RetGC1 complex, GCAP1-GFP had to be in an excess over RetGC1 such that the concentration of GCAP1-GFP in the cell that is not bound to the RetGC1 had to be high enough to saturate RetGC1. At the same time, we could not express a large excess of the tagged GCAP1 over RetGC1, because a high background of free GCAP1-GFP reduces the accuracy of the measurement in its membrane-associated fraction containing dsRed-tagged RetGC1. Therefore, we had to increase the proportion of the GCAP1-expressing construct in the cotransfection mixture until the relative fluorescence intensity of the free GCAP1-GFP in the nucleus became higher than ~25% of its maximal fluorescence in the cell (thus indicating that the GCAP−RetGC1 binding approached saturation) yet was still within the proportional range for PMU sensitivity. Since the free GCAP1-GFP is distributed evenly throughout the cell (*32*), the fluorescence intensity of GCAP1-GFP in the nuclei reflected the concentration of free GCAP1-GFP in the cell. Therefore, subtracting the GCAP1-GFP fluorescence level in the nucleus from that in the endoplasmic reticulum gives the net fluorescence value for GCAP1-GFP colocalized with the dsRed-RetGC1 species and allows us to calculate the ratio between the two fluorescent tags in comparison with the 1:1 chimera standard (Figure 5C). For wild-type RetGC1, this ratio was 1.6 ± 0.06 (mean ± standard error of the mean; $n = 61$), which in comparison with the ratio of 1.87 for the standard yields a GCAP1:RetGC1 ratio in the complex of 0.86:1, strongly suggesting their 1:1 stoichiometry.

The fluorescence ratio between the two tags associated with the membranes versus the levels of the free GCAP1-GFP fluorescence was also fitted with a fractional saturation curve (Figure 5D). In comparison with the 1:1 standard chimera, a value of 1.01 was found for the molar ratio between the two proteins at saturation. We would also like to point out that the GFP and the dsRed tags in the chimera and in the GCAP1−RetGC complex are located on the opposite sides of the transmembrane domain of RetGC; hence, they are separated by the minimal distance equal to the thickness of the membrane (*39*) and very likely even farther apart, because GCAP1 in HEK293 cells is not directly anchored by the membrane bilayer surface (Figures 3 and 4). Therefore, the efficiency of a fluorescence resonance energy transfer between the GFP and dsRed tags (*40*), which is inversely proportional to the sixth power of the distance between them, if any, should be very low and should not affect the results.

The important conclusion from those experiments was that wild-type RetGC1 and GCAP1 formed an equimolar complex when produced in HEK293 cells. Since two catalytic domains are required to form the active center of the cyclase (*29*, *30*), RetGC1 is most likely a dimer (although the existence of higher-order complexes cannot be completely excluded at this point).

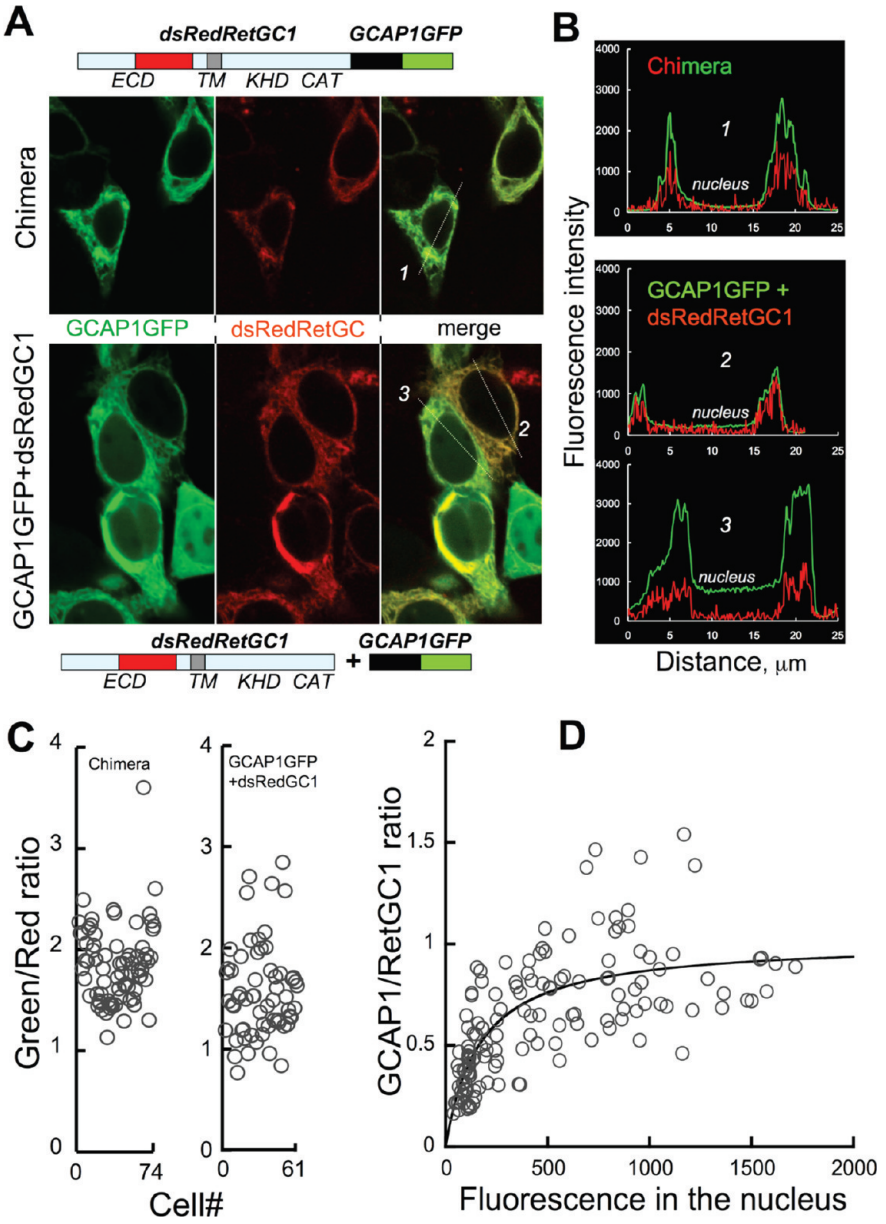

FIGURE 5: Stoichiometry of GCAP1−RetGC1 binding in HEK293 cells. (A) eGFP-tagged GCAP1 and a monomeric dsRed-tagged RetGC1 were fused together as a single polypeptide containing both fluorescently tagged proteins (1:1 chimera standard): *ECD*, extracellular domain; *TM*, transmembrane domain; *KHD*, kinase homology domain; *CAT*, catalytic domain. The top three panels show the fluorescence of the eGFP and dsRed tags in the chimera-expressing HEK293 cells. The 1:1 chimera exhibited strictly membrane localization (primarily ER), indistinguishable from that of dsRed-tagged RetGC1 (*32*). The bottom three panels show the fluorescence of the eGFP and dsRed tags and their merged image in the cells that coexpressed a mixture of GCAP1-GFP and dsRed-RetGC1 cDNAs. (B) Example of fluorescence intensity profiles recorded from the cells expressing the 1:1 chimera (cell #1) or coexpressing individual GCAP1-GFP and dsRed-RetGC1 species (cells #2 and #3) shown in panel A. Subtracting the GCAP1-GFP fluorescence level in the nucleus ("free GCAP1-GFP") from that in the endoplasmic reticulum yields the net fluorescence value for GCAP1-GFP colocalized with dsRed-RetGC1. (C) Ratio between GFP and dsRed tag fluorescence in HEK293 cells that expressed the 1:1 chimera standard (left) or a mixture of the individual GCAP1-GFP and dsRed −RetGC1 species. In the latter case (right), the ratio was plotted for the cells where the GCAP1-GFP fluorescence in the nucleus exceeded 10% of the proportional PMA range maximum [GFP levels of >450 (see panel B for an example)]. Each point represents a separate cell. (D) GCAP1:RetGC1 molar ratio calculated from the fluorescence ratio of their two tags divided by that of the 1:1 chimera standard. The data points were fitted using the fractional saturation function $R = R_{max} \times F/(F + F_{1/2})$, where R is the molar ratio between membrane-associated GCAP1-GFP and dsRed-RetGC1, R_{max} is the R value at saturation by GCAP1-GFP, F is the GCAP1-GFP fluorescence level in the nucleus (free GCAP-GFP), and $F_{1/2}$ is the F value corresponding to half-saturation by GCAP1-GFP. Each point represents a separate cell. All measurements were conducted using the same settings for excitation and image acquisition.

Therefore, our experiments argue that each dimer of RetGC1 must contain two GCAP1 molecules, one per each RetGC1 subunit. These results also argue that since both D639Y and R768W mutants failed to "anchor" GCAP1 to the membranes (Figure 3), each of them was unable to bind and recruit the single molecule of GCAP1 required to produce their 1:1 complex, such as with wild-type RetGC1.

Since the RetGC1−GCAP1 complex is likely to be a hetero-tetramer consisting of two RetGC1 and two GCAP1 molecules, could the effect of both mutations in RetGC1 be dominant negative, with the mutant RetGC1 being able to abolish the activity of wild-type RetGC1 as a result of their interaction? We tested the activity of wild-type RetGC1 coexpressed with each mutant. In that case, however, it was challenging to reliably

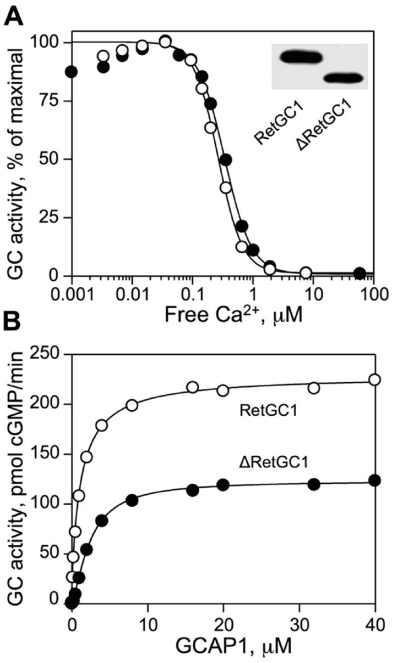

FIGURE 6: Properties of ΔRetGC1. (A) Ca^{2+} sensitivity of wild-type RetGC1 and ΔRetGC1 stimulated by 10 μM recombinant GCAP1 in the presence of 1 mM free Mg^{2+}. The data were fitted as fractional activity of RetGC1 by the function $Y = 100\%/[1 + ([Ca]_f/[Ca]_{1/2})^n]$, where $[Ca]_{1/2}$ is the free Ca^{2+} concentration required for half-maximal inhibition of RetGC1 and n is the cooperativity coefficient. The inset shows the Western blot analysis of HEK293 membranes from the cells expressing wild-type RetGC1 and ΔRetGC1 using RetGC1Cat antibody produced against the catalytic domain of RetGC1. (B) Activation of wild-type RetGC1 and ΔRetGC1 by purified GCAP1 in the presence of 1 mM EGTA and 1 mM free Mg^{2+}. The data were fitted by the equation $A = A_{max} \times [GCAP]^n/(K_{1/2}{}^n + [GCAP]^n)$, where A is the activity of guanylyl cyclase in the assay, A_{max} is the maximal activity of guanylyl cyclase, [GCAP] is the concentration of GCAP1, $K_{1/2}$ is the concentration of GCAP1 required for half-maximal activation of RetGC1, and n is the cooperativity coefficient. The activity of RetGC1 in each assay was equalized per RetGC1 content of the wild type. For other conditions of the assay, see Experimental Procedures.

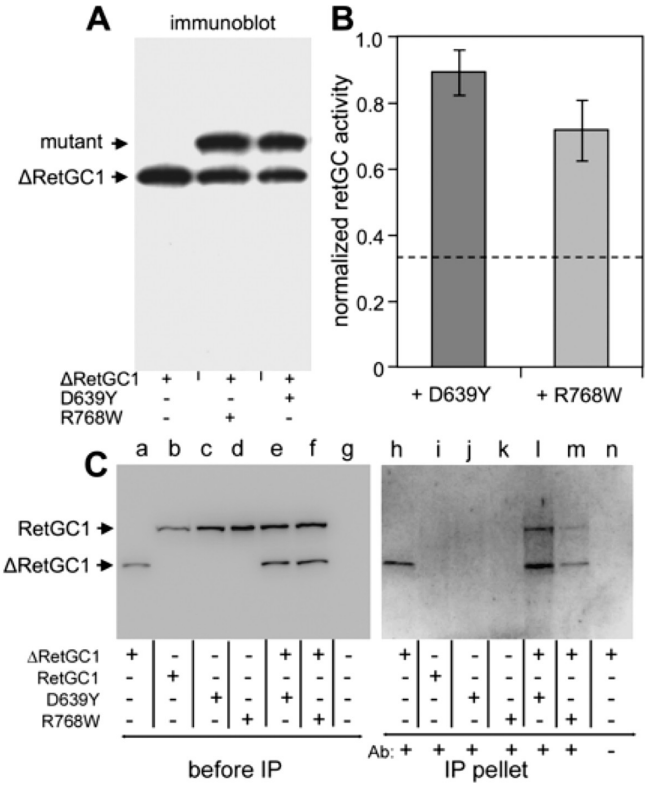

FIGURE 7: Effects of the ΔRetGC1 coexpression with D639Y and R768W mutants in HEK293 cells. (A) Immunoblotting of HEK293 membranes from the cells coexpressing ΔRetGC1 and D639Y or R768W mutants using antibodies produced against the catalytic domain of RetGC1. (B) Guanylyl cyclase activity of ΔRetGC1 in HEK293 cells coexpressing ΔRetGC1 and D639Y or R768W mutants. The cyclase activity was normalized to that of ΔRetGC1 expressed alone. The average of three independent measurements is shown. (C) Co-immunoprecipitation (co-IP) of the D639Y and R768W mutants with the Myc-tagged ΔRetGC1. The left panel (lanes a−g) shows immunoblotting of RetGC1 variants expressed in HEK293 membranes used in the co-IP experiments (no further normalization per RetGC1 content between the preparations was done for the experiments); lane g shows nontransfected cells. The membranes were then dissolved in the extraction buffer and processed for immunoprecipitation with anti-Myc antibody as described in Experimental Procedures. The right panel (lanes h−n) shows the immunoblot of the fractions recovered from the beads after anti-Myc antibody precipitation (the blot was probed with the RetGC1Cat antibody). The higher background in the right panel was due to the longer exposure time needed to visualize the immunoprecipitated proteins recovered from the beads. Notice that both D639Y and R768W are precipitated only when coexpressed with ΔRetGC1 (lanes l and m), but not when expressed separately (lanes j and k). In lane n, the anti-Myc antibody was omitted from the co-IP mixture as a negative control for the ΔRetGC1 precipitation in lane h. All samples were processed simultaneously in the same experiment.

measure the ratio between the mutant and nonmutant cyclase from the immunoblotting; our antibodies produced against either the catalytic or the kinase homology domain of the cyclase do not discriminate between the wild type and any of the mutants. Therefore, we removed an ~20 kDa fragment from the cyclase extracellular domain [the same region that can be substituted with the dsRed tag (*32*)] with a short peptide fragment containing the EQKLISEEDL myc tag. That modification (ΔRetGC1) did not alter the Ca^{2+}/GCAP1 sensitivity of the cyclase regulation (Figure 6A), only slightly reduced the maximal activity of the cyclase (Figure 6A), and did not dramatically affect the apparent affinity of the shortened RetGC1 for GCAP1 in vitro (Figure 6B). At the same time, it made the shortened wild-type ΔRetGC1 easily distinguishable from the normal-size D639Y and R768W mutants when each mutant and the ΔRetGC1 were coexpressed in the same cells (Figure 6A, inset).

We reasoned that if both ΔRetGC1 and one of each of the mutants are coexpressed at an equimolar ratio and are capable of forming a RetGC1 heterodimer, then on average one-third of the ΔRetGC1 produced in the culture was expected to remain a homodimer whereas two-thirds would remain to form a heterodimer with the mutant. Neither D639Y nor R768W alone displays any GCAP1-stimulated activity (Figure 2); therefore, if either mutation had a strong dominant negative effect, one could expect that only the one-third of the ΔRetGC1 remaining as the homodimer would retain its activity. In contrast, Figure 7B demonstrates that the activity of ΔRetGC1 coexpressed with each mutant was only modestly reduced compared to the activity of ΔRetGC1 expressed alone and remained well above the level expected for a strong dominant negative effect (dashed line).

A possible explanation for the lack of a dominant negative effect for both the D639Y and R768W mutations in Figure 7B could be merely their complete inability to dimerize with the wild-type counterpart. However, the results shown in Figure 7C demonstrate that both D639Y and R768W RetGC1 can

co-immunoprecipitate with ΔRetGC1 (lanes l and m, vs lanes j and k) by the antibody that recognizes the Myc tag incorporated into the shortened extracellular domain of ΔRetGC1 (lanes a and h), absent from full-length RetGC1 (lanes b−d and i−k). Since the immunoprecipitation in our experiments could be conducted only with a detergent-solubilized RetGC1, a procedure that completely inactivates its regulation by GCAPs (ref *41* and our unpublished observations) and cannot provide sufficiently quantitative characterization of the dimerization efficiency, we cannot rule out the possibility that dimerization of the mutants with the normal RetGC1 is indeed affected. However, the fact that both RetGC1 mutants were clearly able to co-IP with ΔRetGC1 in these experiments would rather argue that the mutant cyclase does not lack the ability to associate with the normal gene product in vivo.

To summarize, our findings strongly argue that RetGC1 affected by either of the two LCA-associated mutations cannot bind GCAP1. At the same time, neither of the two mutations was able to abolish the activity of the normal RetGC1 when co-expressed in the same cell (and likely even despite forming a dimer with the unaffected cyclase). The lack of a strong dominant negative effect for each mutant would appear consistent with one of the subjects in the original clinical study who carried the heterozygous D639Y mutation not developing the severe loss of both rod and cone function typical of LCA [although, like with some other mutations in the GUCY2D gene (*42*), had subclinical change in cone responses to light (B. Falsini, personal communication)], despite that the primary binding (i.e., "docking") of GCAP1 on the mutated RetGC1 molecule itself was completely abolished. Therefore, it is most likely that both mutants characterized in this study can affect photoreceptor viability leading to the LCA symptoms, but propagation of its potential effect would also require additional, currently unidentified, genetic interactions.

This study also demonstrates that our recently developed cell-based assay for binding of GCAP1 to RetGC1 (*32*) allows identification of the residues involved in the GCAP1−RetGC1 docking event. They show that the docking of GCAP1 on the cyclase can be completely prevented by a single-amino acid substitution, such as D639Y or R768W, affecting the KHD domain of RetGC1. A peptide containing D639 was previously found among the products of RetGC1 chemical cross-linking with GCAP1 in vitro (*43*), although it was not clear at that time whether that product reflected the primary binding of GCAP1 to the cyclase or their secondary regulatory interactions, which may potentially involve different sites (*44*). Together with the chemical cross-linking data (*43*), our functional experiments now directly implicate the region containing the D639 residue in the primary binding (docking) of GCAP1. In addition to that, the part of the RetGC1 KHD domain containing R768 was never before suspected to participate in the RetGC1−GCAP1 docking interactions. Therefore, using fluorescently tagged RetGC1 and GCAP1 in living cells opens a possibility for more accurate identification of the sites required for their docking.

ACKNOWLEDGMENT

We thank Dr. B. Falsini and Dr. J. Nathans for their generous gift of the original samples from the LCA patients used in this study.

SUPPORTING INFORMATION AVAILABLE

Schematics of the chimera construct and immunoblotting of the HEK293 membrane fraction isolated from cells expressing wild-type RetGC1, the dsRed-RetGC1−GCAP1-GFP chimera, or dsRed-RetGC1 (as indicated above each lane) probed with RetGC1Cat, anti-GFP, or anti-GCAP1 (*32*) antibody (top blots) or with RetGC1Cat, anti-GFP, and anti-dsRed RFP antibody (bottom blots) (Figure 1S). This material is available free of charge via the Internet at http://pubs.acs.org.

REFERENCES

1. Pugh, E. N., Jr., Duda, T., Sitaramayya, A., and Sharma, R. K. (1997) Photoreceptor guanylate cyclases: A review. *Biosci. Rep. 17*, 429–473.
2. Hodgkin, A. L., and Nunn, B. J. (1988) Control of light-sensitive current in salamander rods. *J. Physiol. 403*, 439–471.
3. Burns, M. E., Mendez, A., Chen, J., and Baylor, D. A. (2002) Dynamics of cyclic GMP synthesis in retinal rods. *Neuron 36*, 81–91.
4. Koch, K. W., and Stryer, L. (1988) Highly cooperative feedback control of retinal rod guanylate cyclase by calcium ions. *Nature 334*, 64–66.
5. Gorczyca, W. A., Gray-Keller, M. P., Detwiler, P. B., and Palczewski, K. (1994) Purification and physiological evaluation of a guanylate cyclase activating protein from retinal rods. *Proc. Natl. Acad. Sci. U.S.A. 91*, 4014–4018.
6. Dizhoor, A. M., Lowe, D. G., Olshevskaya, E. V., Laura, R. P., and Hurley, J. B. (1994) The human photoreceptor membrane guanylyl cyclase, RetGC, is present in outer segments and is regulated by calcium and a soluble activator. *Neuron 12*, 1345–1352.
7. Peshenko, I. V., and Dizhoor, A. M. (2004) Guanylyl cyclase-activating proteins (GCAPs) are Ca^{2+}/Mg^{2+} sensors: Implications for photoreceptor guanylyl cyclase (RetGC) regulation in mammalian photoreceptors. *J. Biol. Chem. 279*, 16903–16906.
8. Gray-Keller, M. P., and Detwiler, P. B. (1994) The calcium feedback signal in the phototransduction cascade of vertebrate rods. *Neuron 13*, 849–861.
9. Woodruff, M. L., Sampath, A. P., Matthews, H. R., Krasnoperova, N. V., Lem, J., and Fain, G. L. (2002) Measurement of cytoplasmic calcium concentration in the rods of wild-type and transducin knockout mice. *J. Physiol. 542*, 843–854.
10. Peshenko, I. V., and Dizhoor, A. M. (2007) Activation and inhibition of photoreceptor guanylyl cyclase by guanylyl cyclase activating protein 1 (GCAP-1): The functional role of Mg^{2+}/Ca^{2+} exchange in EF-hand domains. *J. Biol. Chem. 282*, 21645–21652.
11. Makino, C. L., Peshenko, I. V., Wen, X. H., Olshevskaya, E. V., Barrett, R., and Dizhoor, A. M. (2008) A role for GCAP2 in regulating the photoresponse. Guanylyl cyclase activation and rod electrophysiology in GUCA1B knock-out mice. *J. Biol. Chem. 283*, 29135–29143.
12. Lowe, D. G., Dizhoor, A. M., Liu, K., Gu, Q., Spencer, M., Laura, R., Lu, L., and Hurley, J. B. (1995) Cloning and expression of a second photoreceptor-specific membrane retina guanylyl cyclase (RetGC), RetGC-2. *Proc. Natl. Acad. Sci. U.S.A. 92*, 5535–5539.
13. Yang, R. B., Foster, D. C., Garbers, D. L., and Fulle, H. J. (1995) Two membrane forms of guanylyl cyclase found in the eye. *Proc. Natl. Acad. Sci. U.S.A. 92*, 602–606.
14. Baehr, W., Karan, S., Maeda, T., Luo, D. G., Li, S., Bronson, J. D., Watt, C. B., Yau, K. W., Frederick, J. M., and Palczewski, K. (2007) The function of guanylate cyclase 1 and guanylate cyclase 2 in rod and cone photoreceptors. *J. Biol. Chem. 282*, 8837–8847.
15. Yang, R. B., Robinson, S. W., Xiong, W. H., Yau, K. W., Birch, D. G., and Garbers, D. L. (1999) Disruption of a retinal guanylyl cyclase gene leads to cone-specific dystrophy and paradoxical rod behavior. *J. Neurosci. 19*, 5889–5897.
16. Dizhoor, A. M., Olshevskaya, E. V., Henzel, W. J., Wong, S. C., Stults, J. T., Ankoudinova, I., and Hurley, J. B. (1995) Cloning, sequencing, and expression of a 24-kDa Ca^{2+}-binding protein activating photoreceptor guanylyl cyclase. *J. Biol. Chem. 270*, 25200–25206.
17. Gorczyca, W. A., Polans, A. S., Surgucheva, I. G., Subbaraya, I., Baehr, W., and Palczewski, K. (1995) Guanylyl cyclase activating protein. A calcium-sensitive regulator of phototransduction. *J. Biol. Chem. 270*, 22029–22036.
18. Mendez, A., Burns, M. E., Sokal, I., Dizhoor, A. M., Baehr, W., Palczewski, K., Baylor, D. A., and Chen, J. (2001) Role of guanylate cyclase-activating proteins (GCAPs) in setting the flash sensitivity of rod photoreceptors. *Proc. Natl. Acad. Sci. U.S.A. 98*, 9948–9953.
19. Stephen, R., Filipek, S., Palczewski, K., and Sousa, M. C. (2008) Ca^{2+}-dependent regulation of phototransduction. *Photochem. Photobiol. 84*, 903–910.

20. Imanishi, Y., Li, N., Sokal, I., Sowa, M. E., Lichtarge, O., Wensel, T. G., Saperstein, D. A., Baehr, W., and Palczewski, K. (2002) Characterization of retinal guanylate cyclase-activating protein 3 (GCAP3) from zebrafish to man. *Eur. J. Neurosci. 15*, 63–78.
21. Perrault, I., Rozet, J. M., Calvas, P., Gerber, S., Camuzat, A., Dollfus, H., Chatelin, S., Souied, E., Ghazi, I., Leowski, C., Bonnemaison, M., Le Paslier, D., Frezal, J., Dufier, J. L., Pittler, S., Munnich, A., and Kaplan, J. (1996) Retinal-specific guanylate cyclase gene mutations in Leber's congenital amaurosis. *Nat. Genet. 14*, 461–464.
22. Perrault, I., Rozet, J. M., Gerber, S., Ghazi, I., Ducroq, D., Souied, E., Leowski, C., Bonnemaison, M., Dufier, J. L., Munnich, A., and Kaplan, J. (2000) Spectrum of RetGC1 mutations in Leber's congenital amaurosis. *Eur. J. Hum. Genet. 8*, 578–582.
23. Duda, T., Venkataraman, V., Goraczniak, R., Lange, C., Koch, K. W., and Sharma, R. K. (1999) Functional consequences of a rod outer segment membrane guanylate cyclase (ROS-GC1) gene mutation linked with Leber's congenital amaurosis. *Biochemistry 38*, 509–515.
24. Dharmaraj, S. R., Silva, E. R., Pina, A. L., Li, Y. Y., Yang, J. M., Carter, C. R., Loyer, M. K., El-Hilali, H. K., Traboulsi, E. K., Sundin, O. K., Zhu, D. K., Koenekoop, R. K., and Maumenee, I. H. (2000) Mutational analysis and clinical correlation in Leber congenital amaurosis. *Ophthalmic Genet. 21*, 135–150.
25. Tucker, C. L., Ramamurthy, V., Pina, A. L., Loyer, M., Dharmaraj, S., Li, Y., Maumenee, I. H., Hurley, J. B., and Koenekoop, R. K. (2004) Functional analyses of mutant recessive GUCY2D alleles identified in Leber congenital amaurosis patients: Protein domain comparisons and dominant negative effects. *Mol. Vision 10*, 297–303.
26. Rozet, J. M., Perrault, I., Gerber, S., Hanein, S., Barbet, F., Ducroq, D., Souied, E., Munnich, A., and Kaplan, J. (2001) Complete abolition of the retinal-specific guanylyl cyclase (RetGC-1) catalytic ability consistently leads to leber congenital amaurosis (LCA). *Invest. Ophthalmol. Visual Sci. 42*, 1190–1192.
27. Kelsell, R. E., Gregory-Evans, K., Payne, A. M., Perrault, I., Kaplan, J., Yang, R. B., Garbers, D. L., Bird, A. C., Moore, A. T., and Hunt, D. M. (1998) Mutations in the retinal guanylate cyclase (RetGC-1) gene in dominant cone-rod dystrophy. *Hum. Mol. Genet. 7*, 1179–1184.
28. Perrault, I., Rozet, J. M., Gerber, S., Kelsell, R. E., Souied, E., Cabot, A., Hunt, D. M., Munnich, A., and Kaplan, J. (1998) A RetGC-1 mutation in autosomal dominant cone-rod dystrophy. *Am. J. Hum. Genet. 63*, 651–654.
29. Tucker, C. L., Woodcock, S. C., Kelsell, R. E., Ramamurthy, V., Hunt, D. M., and Hurley, J. B. (1999) Biochemical analysis of a dimerization domain mutation in RetGC-1 associated with dominant cone-rod dystrophy. *Proc. Natl. Acad. Sci. U.S.A. 96*, 9039–9044.
30. Ramamurthy, V., Tucker, C., Wilkie, S. E., Daggett, V., Hunt, D. M., and Hurley, J. B. (2001) Interactions within the coiled-coil domain of RetGC-1 guanylyl cyclase are optimized for regulation rather than for high affinity. *J. Biol. Chem. 276*, 26218–26229.
31. Peshenko, I. V., Moiseyev, G. P., Olshevskaya, E. V., and Dizhoor, A. M. (2004) Factors that determine Ca^{2+} sensitivity of photoreceptor guanylyl cyclase. Kinetic analysis of the interaction between the Ca^{2+}-bound and the Ca^{2+}-free guanylyl cyclase activating proteins (GCAPs) and recombinant photoreceptor guanylyl cyclase 1 (RetGC-1). *Biochemistry 43*, 13796–13804.
32. Peshenko, I. V., Olshevskaya, E. V., and Dizhoor, A. M. (2008) Binding of guanylyl cyclase activating protein 1 (GCAP1) to retinal guanylyl cyclase (RetGC1). The role of individual EF-hands. *J. Biol. Chem. 283*, 21747–21757.
33. Peshenko, I. V., and Dizhoor, A. M. (2006) Ca^{2+} and Mg^{2+} binding properties of GCAP-1. Evidence that Mg^{2+}-bound form is the physiological activator of photoreceptor guanylyl cyclase. *J. Biol. Chem. 281*, 23830–23841.
34. Laura, R. P., Dizhoor, A. M., and Hurley, J. B. (1996) The membrane guanylyl cyclase, retinal guanylyl cyclase-1, is activated through its intracellular domain. *J. Biol. Chem. 271*, 11646–11651.
35. Olshevskaya, E. V., Hughes, R. E., Hurley, J. B., and Dizhoor, A. M. (1997) Calcium binding, but not a calcium-myristoyl switch, controls the ability of guanylyl cyclase-activating protein GCAP-2 to regulate photoreceptor guanylyl cyclase. *J. Biol. Chem. 272*, 14327–14333.
36. Camuzat, A., Rozet, J. M., Dollfus, H., Gerber, S., Perrault, I., Weissenbach, J., Munnich, A., and Kaplan, J. (1996) Evidence of genetic heterogeneity of Leber's congenital amaurosis (LCA) and mapping of LCA1 to chromosome 17p13. *Hum. Genet. 97*, 798–801.
37. Yzer, S., Leroy, B. P., De Baere, E., de Ravel, T. J., Zonneveld, M. N., Voesenek, K., Kellner, U., Ciriano, J. P., de Faber, J. T., Rohrschneider, K., Roepman, R., den Hollander, A. I., Cruysberg, J. R., Meire, F., Casteels, I., van Moll-Ramirez, N. G., Allikmets, R., van den Born, L. I., and Cremers, F. P. (2006) Microarray-based mutation detection and phenotypic characterization of patients with Leber congenital amaurosis. *Invest. Ophthalmol. Visual Sci. 47*, 1167–1176.
38. Hwang, J. Y., Lange, C., Helten, A., Hoppner-Heitmann, D., Duda, T., Sharma, R. K., and Koch, K. W. (2003) Regulatory modes of rod outer segment membrane guanylate cyclase differ in catalytic efficiency and Ca^{2+}-sensitivity. *Eur. J. Biochem. 270*, 3814–3821.
39. Heller, H., Schaefer, M., and Schulten, K. (1993) Molecular dynamics simulation of a bilayer of 200 lipids in the gel and in the liquid-crystal phases. *J. Phys. Chem. 97*, 8343–8360.
40. Van der Krogt, G. N., Ogink, J., Ponsioen, B., and Jalink, K. (2008) A comparison of donor-acceptor pairs for genetically encoded FRET sensors: Application to the Epac cAMP sensor as an example. *PLoS One 3*, e1916.
41. Koch, K. W. (1991) Purification and identification of photoreceptor guanylate cyclase. *J. Biol. Chem. 266*, 8634–8637.
42. Koenekoop, R. K., Fishman, G. A., Iannaccone, A., Ezzeldin, H., Ciccarelli, M. L., Baldi, A., Sunness, J. S., Lotery, A. J., Jablonski, M. M., Pittler, S. J., and Maumenee, I. (2002) Electroretinographic abnormalities in parents of patients with Leber congenital amaurosis who have heterozygous GUCY2D mutations. *Arch. Ophthalmol. 120*, 1325–1330.
43. Krylov, D. M., and Hurley, J. B. (2001) Identification of proximate regions in a complex of retinal guanylyl cyclase 1 and guanylyl cyclase-activating protein-1 by a novel mass spectrometry-based method. *J. Biol. Chem. 276*, 30648–30654.
44. Duda, T., Fik-Rymarkiewicz, E., Venkataraman, V., Krishnan, R., Koch, K. W., and Sharma, R. K. (2005) The calcium-sensor guanylate cyclase activating protein type 2 specific site in rod outer segment membrane guanylate cyclase type 1. *Biochemistry 44*, 7336–7345.